Structural properties of undoped and doped cubic GaN grown on SiC(001)

E. Martinez-Guerrero,[a] E. Bellet-Amalric, L. Martinet, G. Feuillet, and B. Daudin
Département de la Recherche Fondamentale sur la Matière Condensée, SP2M CEA/38054 Grenoble, France

H. Mariette[b]
Laboratoire de Spectrometrie Physique, University Joseph Fourier, Grenoble I, CNRS, France

P. Holliger
Laboratoire d'Electronique et Technologie de l'Information DMEL/SCPM, CEA/Grenoble, France

C. Dubois and C. Bru-Chevallier
Laboratoire de Physique de la Matière, INSA Lyon, CNRS, France

P. Aboughe Nze, T. Chassagne, G. Ferro, and Y. Monteil
Laboratoire de Multimatériaux et Interfaces, University Claude Bernard, Lyon I CNRS, France

(Received 19 July 2001; accepted for publication 11 January 2002)

Transmission electron microscopy and x-ray diffraction measurements reveal the presence of stacking faults (SFs) in undoped cubic GaN thin layers. We demonstrate the importance of the defects in the interfacial region of the films by showing that the SFs act as nucleation sites for precipitates of residual impurities such as C and Si present in the GaN layers grown on SiC(001) substrates. We used the imaging secondary ion mass spectroscopy technique to locate these impurities. The systematic decrease of the SF density as a function of the layer thickness is explained by an annihilation mechanism. Finally, the effects of usual dopants on the structural properties of GaN layers are discussed. It is shown that Mg has a tendency to incorporate out of the Ga site by forming Mg precipitates for a concentration higher than 10^{19} cm^{-3} in contrast with the results found for heavily Si doped layers. © *2002 American Institute of Physics.*
[DOI: 10.1063/1.1456243]

INTRODUCTION

III–nitrides are very promising semiconductors for their applications in optoelectronics, high temperature, and high speed devices. It has been demonstrated that these materials can crystallize in the wurzite structure or in the zinc blende structure. Most studies have been devoted to the wurzite structure, stimulated by the realization of blue and violet laser diodes, operating at room temperature.[1] However optical properties of GaN crystallized in the zinc blende structure (*c*-GaN), which exhibits higher crystallographic symmetry, are expected to present some advantages compared to the hexagonal phase due to the absence of an internal electric field. In addition, the possibility of an electronic integration with GaAs or Si devices, makes cubic GaN very attractive. However, due to the difficulty in growing this metastable phase of GaN, a relatively limited amount of work has been devoted to the growth of *c*-GaN and to the fabrication of light emitting diodes.[2–4] Among the remaining problems which hinder further progress, the influence of extended defects on the structural and electrical properties and also the apparent lack of understanding of the mechanisms underlying impurity incorporation are of major importance. The high concentration of defects which often dominates the optical and electrical characteristics, a consequence of the lack of adapted substrates, makes the reproducibility of devices difficult. Indeed, the major limitation in the growth of *c*-GaN originates from polytypism, i.e., a tendency to form hexagonal subdomains within the cubic crystal.

As it has been revealed by several experimental studies, the (111) stacking faults (SFs) are the predominant crystallographic defects in cubic III–nitrides.[5–7] Along these lines, combined with the experimental observation that thin layers exhibit a high mosaicity as seen by x-ray diffraction (XRD), this suggests that the SFs are responsible for the degradation of the structural quality of these materials. Although it is not clear how or whether the interaction of impurities (or point defects) with SFs may affect the electronic properties, recent theoretical calculations suggest that impurities have a tendency to segregate towards the SFs,[8] similar to the well known segregation phenomena into the core of dislocations. In this case, regions near the layer/substrate interface would be conductive. In fact the defective interfacial region of the films generally exhibits higher residual impurity concentration than the rest of the film,[9] most likely due to outdiffusion from the substrate. In this work we provide evidence that SFs act as nucleation sites for precipitates of residual impurities. In general the thicker the buffer layer, the lower the SF density. Consequently, a thick buffer layer is required to avoid the effects of the interfacial defects.

Moreover, to fabricate GaN-based devices, the control of doping with intentional impurities is desirable. *n*-type doping of *c*-GaN with Si is currently performed.[10,11] By contrast, *p*-type doping of *c*-GaN layers presents many more difficulties: the chemical concentration roughly follows the Mg flux,

[a]Author to whom correspondence should be addressed; electronic mail: martinez@cea.fr
[b]Electronic mail: hmariette@cea.fr

but the hole concentration deviates strongly from it, showing the difficulty of incorporating Mg into the Ga site. In addition, as grown *c*-GaN/SiC in our molecular beam epitaxy (MBE) system is *n* type with a background concentration on the order of 10^{18} cm^{-3}. Then, the achievement of *p* type requires an overcompensation of such background electron concentration present in the samples. Nevertheless, high Mg concentration induces a degradation of structural properties associated with an increased mosaicity of doped layers in contrast with the results found for heavy Si doped layers. These results are discussed in the present work in order to identify the limitations of *p* doping of *c*-GaN layers.

EXPERIMENT

The samples under study were grown by MBE on 3C–SiC/Si pseudosubstrates grown by chemical vapor deposition. These substrates have a thickness of 3 μm with a roughness of 5 nm over 20 m. The doped samples were 0.5–1 μm thick with Mg dopant for the *p* doped type and Si for the *n* type. Both types of doped layers were grown on a 1.5 μm thick undoped GaN/AlN buffer layer. Concentrations measured by secondary ion mass spectroscopy (SIMS) were in the range of 1×10^{17}–2.5×10^{20} cm^{-3} for Mg doped layers and 1×10^{18}–7×10^{19} cm^{-3} for Si doped layers. The SIMS analysis was performed using a CAMECA model IMS-5F. SIMS secondary ion imaging was carried out in the resistive anode encoder (RAE) mode. A primary Cs^+ ion beam with 8 keV energy and 45 nA current was used. The rastering area was 250 μm$\times$250 μm and the analyzed area was 150 μm in diameter. For undoped layers, the thickness has been varied from 0.1 to 4.5 μm. All films were grown under stoichiometric conditions for the Ga and N fluxes. The high resolution x-ray diffractometry (HRXRD) measurements were carried out with a SEIFERT XRD system with a beam concentrator prior to the Ge(220) four-bounce monochromator. For the mosaicity measurements on the (002) reflection, a Ge(220) two-bounce analyzer was inserted in front of the detector. The lattice constants were determined by the extended Bond method. The out of plane lattice parameters $a_\perp$ were measured using a set of symmetric (004) reflections. The in-plane parameters $a_\parallel$ were calculated from the $a_\perp/a_\parallel$ ratio measured by a set of several asymmetric (113), (115), (224), and (333) reflections. The transmission electron microscopy (TEM) measurements were conducted using a JEOL 4000EX microscope operated at 400 kV. The samples for TEM were prepared using the standard sandwich technique which included grinding, polishing, and ion milling. All TEM images were taken in bright field imaging conditions.

RESULTS AND DISCUSSION

Reflection high-energy electron diffraction (RHEED) was used to *in situ* monitor the variations of the in-plane lattice parameter. Figure 1 shows the results for GaN/AlN/SiC stacked layers. One can see an abrupt relaxation of the AlN layer onto the SiC substrate in the first deposited nanometers, followed by a stabilization at a value of about 0.8% with respect to the SiC lattice parameter. However, it is

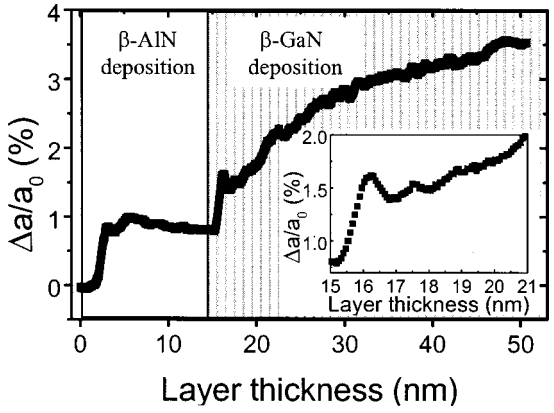

FIG. 1. Strain relaxation of the in-plane lattice parameter of undoped GaN/AlN stacked layers deposited on a 3C–SiC substrate. A thin buffer AlN layer of about 15 nm is used. The break in the *x* axis at 16 nm indicates a growth interruption. The inset corresponds to a zoom of first GaN nanometers deposited onto the AlN layer.

worth noting that the lattice mismatch between both compounds is about 0.3%, based on the lattice parameter values of 3C–SiC[12] and of cubic AlN.[13] Although the origin of the over-relaxation of AlN on 3C–SiC, which is presently observed, is not clear at this stage it is probably due to the generation of extended defects at the interface.[14] When GaN is deposited on AlN, relaxation occurs gradually and is total (2.7%) after about 35 nm. As indicated in the inset of Fig. 1, a peak is observed in the first few nanometers of the GaN layer. This behavior is assigned to the elastic part of the relaxation, i.e., to the formation of small islands of GaN on the AlN surface. It is then followed by a decrease and after that a slow variation of the GaN lattice constant, which reveals a plastic relaxation by coalescence of the islands and the introduction of structural defect like dislocations.

To elucidate such a behavior, the GaN/AlN/SiC stacked layers were studied by TEM, to try and determine the type of structural defects generated during the relaxation. As shown in Fig. 2(a), a large density of extended defects is always present near the interface. These defects, i.e., SFs, microtwins, and dislocations, are formed to relax the strain due to lattice mismatch present between nitride epitaxial layers and cubic substrates.[5,15] Since in the zinc blende structure the SFs lie on the (111) planes, an annihilation mechanism is possible, when two SFs, lying, for example on the (111) and on the (-1-11) planes intersect and annihilate simultaneously with the creation of a sessile (nonglissile) dislocation[16] aligned along ⟨110⟩ directions. This can explain why the majority of defects can be confined in the region close to the interface. In order to estimate the improvement of crystalline quality when the layer thickness is increased, the number of self-annihilated SFs has been estimated as a function of the GaN layer thickness [see Fig. 2(b)]. A reduction of the SF density by a factor of 5 is obtained after the growth of about 400 nm of GaN. The same behavior occurs on the orthogonal family of (111) planes (not visible in the picture), and so a better crystalline quality is expected for a thickness greater than 400 nm. In order to confirm this result, further analysis such as HRXRD measurements, which allows one to estimate the average structural quality on a larger area, were

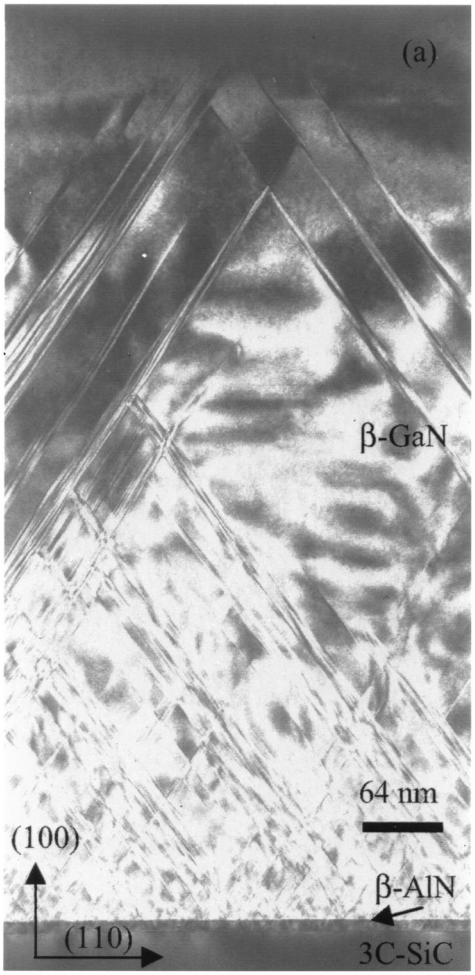

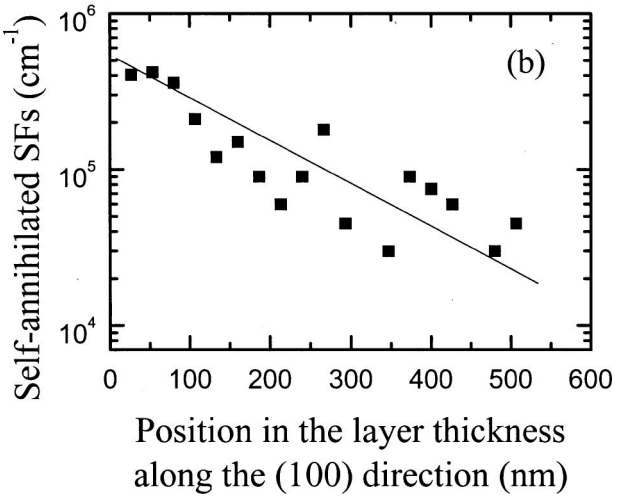

FIG. 2. (a) TEM picture taken from a (110) cross sectional sample of cubic GaN/AlN/SiC stacked layers. SFs along (111) planes are clearly visible. (b) Number of self-annihilated SFs per cm as a function of the layer thickness. [*This measures the number of dislocations lying in the (001) plane in one of the (110) directions.*] Note that an improvement of crystalline quality is obtained for layers thicker than 400 nm.

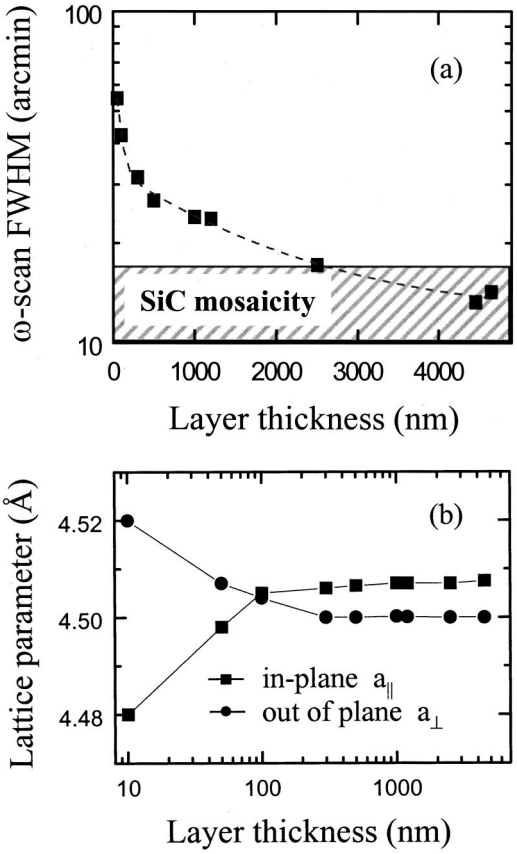

FIG. 3. (a) Thickness dependence of XRD FWHM of (002) diffraction ($\Delta\omega$ in ω scan) for cubic undoped GaN/AlN/SiC layers. (b) Lattice constant variation as a function of the layer thickness.

carried out on these undoped layers. In Fig. 3(a) the full width half maximum (FWHM) of the (002) rocking curve is plotted versus the layer thickness. It evidences a decreasing mosaicity, indicating the improvement of the structural quality with thickness. A value of about 14 arcmin for thick cubic GaN layers is reached as usually reported for the best cubic GaN films.[7,17] This limit is probably imposed by the SiC substrate quality: indeed the mosaicity of these SiC(001) substrates is on the order of 12 ± 5 arcmin.

The relaxation behavior of thick *c*-GaN films has been studied by measuring the variation of both in-plane and out of plane lattice parameters as a function of the layer thickness. The extended Bond method was used to accurately determine the lattice constants. Their variation is plotted in Fig. 3(b). For thin layers, the values of the out of plane lattice parameter $a_{\perp}$ are larger than those of the in-plane parameters $a_{\|}$ indicating a compressive strain. Then, this strain is gradually relieved with the increasing layer thickness. Stable values are reached at about 300 nm, with 4.500 and 4.507 Å for perpendicular and parallel lattice parameters, respectively. For layers thicker than 100 nm, $a_{\|}$ is always larger than $a_{\perp}$, revealing a tensile strain in the *c*-GaN layers. This residual strain of about 0.15% is supposedly related to the thermal mismatch between GaN layers and SiC substrates. However, an accurate determination of the variation of lattice parameters due to the thermal strain is difficult to quantify because the thermal expansion coefficients of *c*-GaN remain unknown.

Turning to the doping issue, our results reveal a clear interaction between structural defects such as the SFs, and impurity incorporation. Figure 4 shows a SIMS profile of

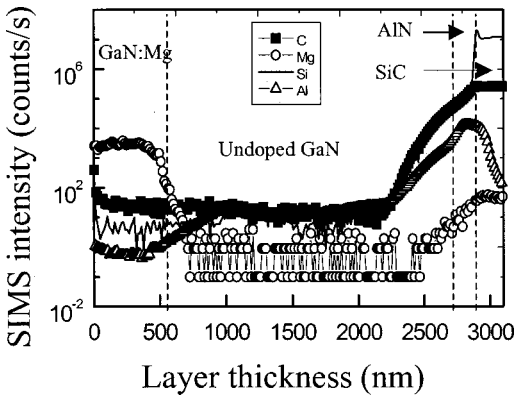

FIG. 4. Open circles (Mg), solid squares (C), solid line (Si), and open triangles (Al) SIMS profiles of Mg doped layers grown on a thick buffer GaN layer.

residual impurities into the GaN layers. The Si, C, and Al impurity profiles decrease below the background signal at a distance of about 500 nm from the GaN/AlN/SiC interface. The presence of C and Si is likely due to the outdiffusion of residual impurities from the SiC substrate. By achieving secondary ions imaging in parallel with SIMS profile measurements, the presence of clusters of Si and C has been clearly evidenced (see Fig. 5). The accurate size of such clusters is difficult to determine because of the divergence of light emitted by the ion clusters. Striking features are observed by following the evolution of such clusters from the top to the bottom of the film as a function of the sputtering time: (i) on the surface and upper layers (i.e., in the Mg doped layer) only a few clusters are present and randomly arranged [Fig. 5(c)]; (ii) their density is slightly increased in the intermediate layers; and finally (iii) in the region near the interface, the cluster density is larger and these clusters are arranged linearly along the ⟨110⟩ directions [Figs. 5(a) and 5(b)]. These directions correspond to the intersection of the (111) planes with the (001) one. Note that the ordering and the high density of the clusters are observed only in the first 500 nm of the GaN buffer layer. Then both the ordering and the density decrease as a function of the thickness from the bottom to the top of the film. This observation suggests that C and Si impurity atoms accumulate in the SF plane up to a distance from the interface for which the majority of SFs are annihilated. The argument of favorable incorporation of impurities into SF sites is supported by some recent calculations that predict a lower segregation energy of these defects as compared to the one for the incorporation in the perfect crystalline environment.[8] Moreover, the incorporation of such impurities in SF sites introduces deeper levels which could act as a pathway of parallel conduction: this would explain why some thin *c*-GaN (or even *c*-AlN!) layers are strongly conductive in agreement with the suggestions of the authors in Ref. 18.

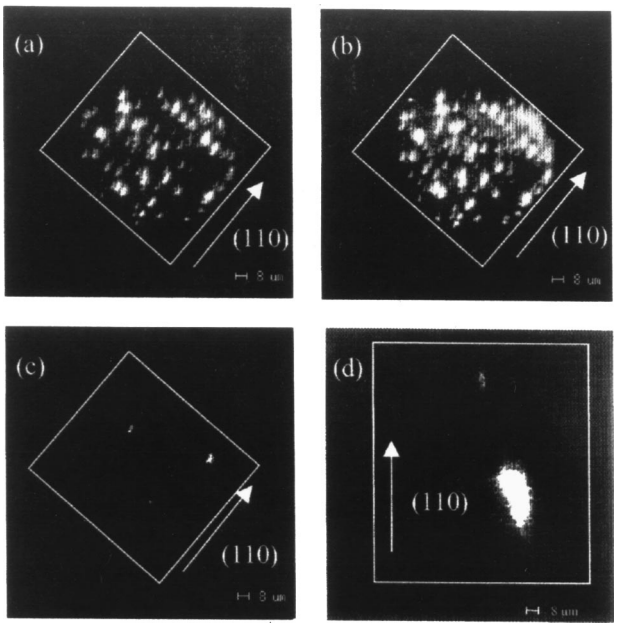

FIG. 5. RAE SIMS images showing precipitates of impurities on Mg doped and buffer layers: C (a) and Si (b) precipitates close to the GaN/SiC interface respectively, C (c) and Mg (d) precipitates close to the surface. A raster area of 250 μm$\times$250 μm on these films was used.

As far as intentional doping is concerned, the incorporation of both Si and Mg impurities gives rise to quite different results. While for *n*-doped GaN layers the electron concentration follows the chemical concentration indicating that most of the Si atoms are electrically active and then are located on the Ga sites[9,10], *p* doping on the other hand, remains a challenge. The latter is probably limited by the background oxygen content present in the layers ($\sim 10^{18}$ cm^{-3}) which requires a high Mg concentration in order to compensate the electron background concentration. The origin of this oxygen concentration is not clear yet: it probably comes from the purity of the Mg source because we observed an increase of the oxygen background by opening the shutter of the Mg cell. Although heavy Mg concentration is obtained in the Mg doped layers, the hole concentration does not vary significantly. Some authors have suggested that this behavior could be related to the formation of Mg complexes like Mg_2, Mg precipitates,[19] or Mg–O complexes[20] that could leave Mg electrically inactive. However, no experimental evidence of such precipitates has yet been reported.

To evaluate the structural quality of the intentionally doped layers, the variation of the mosaicity has been plotted as a function of the chemical concentration of Si and Mg (see Fig. 6). In contrast with results of Xu *et al.*,[21] these measurements do not reveal appreciable degradation for Si incorporation in the whole range of Si concentration. This is in good agreement with the electrical behavior observed for *n*-type doped layers. By contrast, for heavily Mg doped layers ($>2\times10^{19}$ cm^{-3}), an increased mosaicity with increasing Mg concentration is clearly observed. Such results are consistent with the RHEED observations during growth: a spotty RHEED pattern appears when high Mg flux are used, suggesting that Mg atoms limit the surface diffusion of the Ga and N atoms on the growing surface, inducing an increase of the roughness. Then, for a growth under such conditions, the defects density becomes higher. In other words, high Mg concentrations on the growing surface generate nucleation sites of defects which in turn can act as nucleation sites for Mg precipitates as is directly observed by SIMS imaging [see Fig. 5(d)]. Interestingly, the Mg precipitates have a low

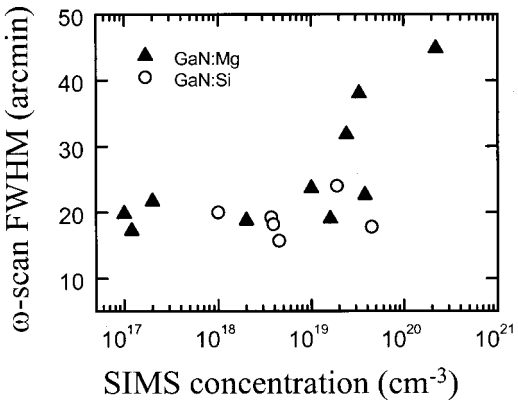

FIG. 6. Mosaicity for: (a) Mg doped layers (solid triangles) and (b) Si doped layers (open circles). Note that for an equivalent thickness (1.5 μm) of undoped GaN layers the mosaicity is about 22 arcmin.

density, about one precipitate per 250 μm$\times$250 μm, and do not follow any arrangement with the crystallographic orientation. This tends to indicate that Mg precipitates do not nucleate on the SF sites like the residual impurities but likely in the Mg-induced defects. Let us also note that no clusters of oxygen were detected.

CONCLUSIONS

In summary we have found that the crystalline quality of thin GaN films is limited by stacking faults generated at the GaN/AlN/SiC interfaces. The improvement of the crystalline quality as a function of the layer thickness is partly due to the annihilation process of the pairs of SF lying on perpendicular (111) planes. We have found that these SFs trap the residual impurities which, thus, act as channels of parasitic conduction in thin cubic GaN layers. For Si doped layers an electrical activation of 100% is obtained. As far as Mg intentionally doped layers are concerned it is clear that, by contrast to the Si incorporation, a Mg doping higher than 10^{19} cm^{-3} leads to a degradation of the crystalline quality of the GaN layers. This can explain why Mg remains mainly electrically inactive.

[1] S. Nakamura, I. Mukai, and M. Senoh, Appl. Phys. Lett. **64**, 1687 (1994).
[2] H. Yang, L. X. Zheng, J. B. Li, X. J. Wang, D. P. Xu, Y. T. Wang, X. W. Hu, and P. D. Han, Appl. Phys. Lett. **74**, 2498 (1999).
[3] D. J. As, A. Richter, J. Busch, M. Lübbers, J. Mimkes, and K. Lischka, Appl. Phys. Lett. **76**, 13 (2000).
[4] H. Gamez-Cuatzin *et al.*, Phys. Status Solidi A **176**, 131 (1999).
[5] A. Trampert, O. Brandt, H. Yang, and K. H. Ploog, Appl. Phys. Lett. **70**, 583 (1997).
[6] H. Okumura, K. Otha, G. Feuillet, K. Balakrishnan, S. Chichibu, H. Hamaguchi, P. Hacke, and S. Yoshida, J. Cryst. Growth **178**, 113 (1997).
[7] D. Wang, Y. Hiroyama, M. Tamura, M. Ichikawa, and S. Yoshida, J. Cryst. Growth **220**, 204 (2000).
[8] T. M. Smidt, J. F. Justo, and A. Fazzio, Appl. Phys. Lett. **78**, 907 (2001).
[9] E. Martinez-Guerrero *et al.*, Mater. Sci. Eng., B **82**, 59 (2001).
[10] D. J. As *et al.*, MRS Internet J. Nitride Semicond. Res. **4S1**, G3.24 (1999).
[11] J. G. Kim, A. C. Frenkel, H. Liu, and R. M. Park, Appl. Phys. Lett. **65**, 91 (1994).
[12] E. Belloti, H.-E. Nilsson, K. F. Brennan, and P. P. Ruden, J. Appl. Phys. **85**, 3211 (1999).
[13] I. Petrov, E. Mojab, R. C. Powell, J. E. Greene, L. Hultman, and J. E. Sundgren, Appl. Phys. Lett. **60**, 2491 (1992).
[14] B. Daudin *et al.*, J. Appl. Phys. **84**, 2295 (1998).
[15] S. Strite, J. Ruan, Z. Li, A. Salvador, H. Chen, D. J. Smith, W. J. Choyke, and H. Morkoç, J. Vac. Sci. Technol. B **9**, 1924 (1991).
[16] G. C. Hua, N. Otsuka, D. C. Grillo, Y. Fan, J. Han, M. D. Ringle, R. L. Gunshor, M. Hovinen, and V. Nurmikko, Appl. Phys. Lett. **65**, 1331 (1994).
[17] H. Okumura *et al.*, J. Cryst. Growth **189/190**, 390 (1998).
[18] D. C. Look, Z. Fang, and L. Polenta, MRS Internet J. Nitride Semicond. Res. **5S1**, W10.5 (2000).
[19] M. S. Brandt, J. W. Ager III, W. Götz, N. M. Johnson, J. S. Harris, Jr., R. J. Molnar, and T. D. Moustakas, Phys. Rev. B **49**, 14758 (1994).
[20] I. Gorczyca, A. Svane, and N. Christensen, Phys. Rev. B **61**, 7494 (2000).
[21] D. Xu, H. Yang, J. B. Li, S. F. Li, Y. T. Wang, D. G. Zhao, and R. H. Wu, J. Cryst. Growth **206**, 150 (1999).